Journal of Solid State Chemistry 182 (2009) 2111–2117

Contents lists available at ScienceDirect

Journal of Solid State Chemistry

journal homepage: www.elsevier.com/locate/jssc

# $\{XW_{12}O_{40}[Cu(en)_2(H_2O)]_3\}$ ($X$ = V, Si): Two novel tri-supported Keggin POMs with transition metal complexes

Yu-Kun Lu, Xiao-Bing Cui, Yan Chen, Jia-Ning Xu, Qing-Bin Zhang, Ya-Bing Liu, Ji-Qing Xu *, Tie-Gang Wang

*College of Chemistry and State Key Laboratory of Inorganic Synthesis and Preparative Chemistry, Jilin University, Changchun, Jilin 130021, P.R. China*

ARTICLE INFO

*Article history:*
Received 21 February 2009
Received in revised form
14 May 2009
Accepted 25 May 2009
Available online 31 May 2009

*Keywords:*
Tri-supported
Polyoxometalates
Transition metal complex
Magnetism
Supramolecular

ABSTRACT

Two novel polyoxometalate derivatives, $\{X^{IV}W_{10}^{VI}W_2^{V}O_{40}[Cu(en)_2(H_2O)]_3\}$ [$X$ = V (**1**), Si (**2**); en- = ethylenediamine], have been hydrothermally synthesized and characterized by elemental analyses, IR, UV–Vis, XPS, EPR, TG and single crystal X-ray diffraction analyses. They represent the first classical Keggin polyoxoanion supported by three transition metal complex moieties, which further act as the neutral molecular unit for the construction of the interesting three-dimensional supramolecular frameworks. The magnetic properties of **1** have also been studied in the temperature range of 4–300 K, and its magnetic susceptibility obeys the Curie–Weiss law, showing antiferromagnetic coupling.



## 1. Introduction

There has been extensive interest in polyoxometalates (POMs), owing to their fascinating properties and great potential applications in many fields (such as catalysis, material science, medicine and magneto chemistry) as well as their unusual structural diversities [1–3]. Since the first POM was discovered about 200 years ago, a number of POMs have increased exponentially, and will probably continue to do so in the coming years. These species gradually grouped into some well-known classes like Keggin-, Wells-Dawson-, Anderson-, Waugh-, Silverton-, Lindquist-type POMs and so on [4–8]. All of these POMs could be named as classical POMs. Recently, the POMs developed at a tremendous rate and a great deal of POMs were discovered, including POMs without any similarity with the classical POMs [9–12] and modified derivatives of the classical POMs [13–32], which could be named as non-classical POMs. In the field of modified POMs, materials based on substituted [13–17], capped [18–23], and supported [24–32] POMs become extraordinarily promising because of their changeable and diverse structures as well as their predominant properties introduced by modifying moieties [1]. Especially, the supported POMs, which is the decoration of polyoxoanions with various organic and/or transition metal complex (TMC) moieties, can be regarded as an ideal atomic level structural model for the determination of the mechanisms of oxide-supported catalysts [1]. Furthermore, such kinds of compounds can be molecularly fine-tuned and provide potentially new types of catalyst systems as well as interesting functional materials with optical, electronic and magnetic properties [1,2].

It is noteworthy that the Keggin-type polyoxoanions have been extensively employed as inorganic building blocks for the construction of modified POMs due to its stability and diverse electronic, photochemical, magnetic and catalytic properties [1]. To the best of our knowledge, a large number of supported POMs constructed from Keggin clusters and TMCs have been hydrothermally synthesized. Typical examples include mono- [24–27], bi- [28,29], tetra- [29–31], penta-supported [32] Keggin structure. Up to now, the study of hetero-POMs is mainly focused on Mo/V/O system [17–23]; in contrast, relatively few tungstovanadate heteropoly complexes have been obtained owing to the kinetic sluggishness of tungsten relative to molybdates and vanadates [30,33–40]. In general, in order to isolate multi-supported POMs, two strategies have been exploited to increase the surface charge density and activate the surface oxygen atoms of heteropolyoxoanions [1]: (I) reduce the metal centers by introducing strong reducing regents [24,29], from $W^{VI}$ to $W^{V}$, for instance; or (II) replace metal centers with another lower-oxidation state metal [24,27–32], for example, from $Mo^{VI}$ to $V^{IV}$. However, usually the highly reduced polyoxoanions are unstable and inclined to be oxidized in ambient atmosphere. Therefore, it is still a great challenge to obtain stable supported POMs. On the basis of the aforementioned points and the continual study of novel

* Corresponding author. Fax: +86 431 85168624.
*E-mail address:* xjq@mail.jlu.edu.cn (J.-Q. Xu).

0022-4596/$ - see front matter © 2009 Elsevier Inc. All rights reserved.
doi:10.1016/j.jssc.2009.05.030

multi-supported POMs, we attempted to explore our research on the preparation of TMCs-supported tungsten–vanadium cluster with strong reducing regents, and we succeed in doing so.

In supported Keggin clusters, linking point of supported complex with cluster can be divided into three situations: (I) terminal-oxygen atom of cluster [24,25,28,29], (II) bridge-oxygen atom of cluster [27] and (III) both terminal- and bridge-oxygen atoms for multi-supported cluster [26,30–32]. In this paper, we report the syntheses, structures, magnetic property and thermal stability of two novel Keggin-type POMs supported by three copper-organonitrogen fragments via bridge oxygen atoms, formulated as $\{XW_{12}O_{40}[Cu(en)_2(H_2O)]_3\}$ [$X$ = V (**1**), Si (**2**)]. As far as we know, the supported Keggin polyoxoanions through bridging-oxygen atoms were infrequently isolated and tri-supported classical Keggin POM possessing discrete structure has not been observed.

## 2. Experimental section

### 2.1. Material and methods

All reagents are used of analytical grade and obtained from commercial sources without further purification. Elemental analyses (C, H and N) were performed on a Perkin-Elmer 2400 CHN elemental analyzer. IR (KBr pellets) spectra were recorded in the 250–4000 $cm^{-1}$ range using a Perkin-Elmer spectrum one spectrophotometer. Determinations of electron paramagnetic resonance (EPR) were carried out on Bruker ER 200D-SRC spectrometer. XPS analyses were performed on thermo ESCALAB 250 spectrometer with an Mg–Ka (1253.6 eV) achromatic X-ray source. Thermogravimetric analyses (TGA) were carried out on a Perkin-Elmer TAG-7 instrument from room temperature to 800 °C with a heating rate of 10 °C/min. Magnetic measurement was obtained using an MPMS-XL5 magnetometer in the temperature range of 4–300 K.

**Table 1**
The crystallographic data for **1** and **2**.

| Compound | **1** | **2** |
|---|---|---|
| Empirical formula | $C_{12}H_{54}Cu_3N_{12}O_{43}VW_{12}$ | $C_{12}H_{54}Cu_3N_{12}O_{43}SiW_{12}$ |
| Formula weight | 3502.34 | 3479.58 |
| Crystal system | trigonal | trigonal |
| Space group | *R*–3*c* | *R*–3*c* |
| $a$ (Å) | 17.9821(4) | 17.959(3) |
| $c$ (Å) | 29.2480(5) | 29.359(6) |
| $\alpha$ (deg) | 90 | 90 |
| $\gamma$ (deg) | 120 | 120 |
| $V$ (Å$^3$) | 8190.4(3) | 8200(2) |
| $Z$ | 6 | 6 |
| $d_{calc}$ (g cm$^{-3}$) | 4.260 | 4.228 |
| Absorption coef. (mm$^{-1}$) | 26.573 | 26.403 |
| $\theta$ range (deg) | 1.91–28.37 | 2.27–26.03 |
| Reflections collected | 18 935 | 22 383 |
| Independent reflections | 2280 | 1808 |
| Completeness | 100.0% | 99.9% |
| Goodness-of-fit on $F^2$ | 1.090 | 1.107 |
| $R$ indexes ($I>2\sigma(I)$)[a] | $R1 = 0.0589$, $wR2 = 0.1450$ | $R1 = 0.0455$, $wR2 = 0.1060$ |
| $R$ (all data)[a] | $R1 = 0.0908$, $wR2 = 0.1620$ | $R1 = 0.0540$, $wR2 = 0.1097$ |
| Largest diff. peak and hole (e/Å$^{-3}$) | 4.271, −3.597 | 3.438, −2.265 |

[a] $R_1 = \Sigma||F_o| - |F_c||/\Sigma|F_o|$; $wR = [\Sigma w(F_o^2 - F_c^2)_2/\Sigma w(F_o^2)^2]^{1/2}$.

**Table 2**
Selected bond lengths (Å) for **1** and **2**.

| Compound **1** | | | | | |
|---|---|---|---|---|---|
| V(1)–O(1) | 1.629(9) | W(1)–O(6) | 1.891(13) | W(2)–O(7)#2 | 1.893(17) |
| V(1)–O(2) | 1.73(3) | W(1)–O(8) | 1.716(8) | W(2)–O(9) | 1.696(8) |
| W(1)–O(1) | 2.349(18) | W(2)–O(1)#1 | 2.455(17) | Cu(1)–N(1) | 2.007(14) |
| W(1)–O(3) | 1.887(3) | W(2)–O(5)#1 | 1.877(16) | Cu(1)–N(2) | 2.028(16) |
| W(1)–O(4) | 1.933(9) | W(2)–O(6) | 1.896(15) | Cu(1)–O(1W) | 2.439(19) |
| W(1)–O(5) | 1.921(12) | W(2)–O(7) | 1.890(17) | Cu(1)–O4 | 2.740 |
| Compound **2** | | | | | |
| Si(1)–O(1) | 1.610(16) | W(1)–O(6) | 1.887(11) | W(2)–O(7)#2 | 1.865(16) |
| Si(1)–O(2) | 1.70(3) | W(1)–O(8) | 1.712(11) | W(2)–O(9) | 1.691(8) |
| W(1)–O(1) | 2.344(16) | W(2)–O(1) | 2.504(15) | Cu(1)–N(1) | 2.007(13) |
| W(1)–O(3) | 1.893(2) | W(2)–O(5) | 1.889(14) | Cu(1)–N(2) | 2.021(14) |
| W(1)–O(4) | 1.928(7) | W(2)–O(6)#1 | 1.883(13) | Cu(1)–O(1W) | 2.430(17) |
| W(1)–O(5) | 1.928(13) | W(2)–O(7) | 1.913(15) | Cu(1)–O4 | 2.752 |

Symmetry codes: for **1** #1 $y$, $x$, $-z+3/2$; #2 $-x+y$, $-x$, $z$. for **2** #1 $y-1/3$, $x+1/3$, $-z+11/6$; #2 $-y+1$, $x-y+1$, $z$.

**Table 3**
Selected bond angles (deg) for **1** and **2**.

| Compound **1** | | | |
|---|---|---|---|
| O(8)–W(1)–O(3) | 100.2(6) | O(9)–W(2)–O(6) | 102.6(8) |
| O(8)–W(1)–O(6) | 101.6(8) | O(5)#1–W(2)–O(6) | 91.1(6) |
| O(3)–W(1)–O(6) | 91.2(6) | O(7)–W(2)–O(6) | 84.0(9) |
| O(8)–W(1)–O(5) | 101.9(9) | O(7)#2–W(2)–O(6) | 156.4(11) |
| O(3)–W(1)–O(5) | 88.7(6) | O(9)–W(2)–O(2)#1 | 155.1(9) |
| O(6)–W(1)–O(5) | 156.1(8) | O(5)#1–W(2)–O(2)#1 | 96.2(8) |
| O(8)–W(1)–O(4) | 99.9(6) | O(7)–W(2)–O(2)#1 | 61.6(9) |
| O(3)–W(1)–O(4) | 159.9(6) | O(6)–W(2)–O(2)#1 | 95.2(8) |
| O(6)–W(1)–O(4) | 86.9(5) | O(9)–W(2)–O(1)#1 | 156.3(6) |
| O(5)–W(1)–O(4) | 85.1(5) | O(5)#1–W(2)–O(1)#1 | 63.3(7) |
| O(8)–W(1)–O(1) | 165.9(6) | O(7)–W(2)–O(1)#1 | 94.3(11) |
| O(3)–W(1)–O(1) | 85.7(6) | O(7)#2–W(2)–O(1)#1 | 95.9(11) |
| O(6)–W(1)–O(1) | 91.0(7) | O(6)–W(2)–O(1)#1 | 62.7(6) |
| O(5)–W(1)–O(1) | 65.2(7) | N(1)#1–Cu(1)–N(1) | 167.3(10) |
| O(4)–W(1)–O(1) | 74.3(6) | N(1)#1–Cu(1)–N(2) | 86.0(6) |
| O(9)–W(2)–O(5)#1 | 100.7(8) | N(1)–Cu(1)–N(2) | 95.0(6) |
| O(9)–W(2)–O(7) | 102.8(10) | N(2)–Cu(1)–N(2)#1 | 171.4(9) |
| O(5)#1–W(2)–O(7) | 156.5(11) | N(1)–Cu(1)–O(1W) | 96.4(5) |
| O(9)–W(2)–O(7)#2 | 100.9(11) | N(2)–Cu(1)–O(1W) | 85.7(4) |
| O(5)#1–W(2)–O(7)#2 | 87.4(9) | O(1)–V(1)–O(1)#2 | 111.0(6) |
| O(7)–W(2)–O(7)#2 | 88.0(11) | O(1)#1–V(1)–O(2) | 107.9(7) |
| Compound **2** | | | |
| O(8)–W(1)–O(6) | 101.9(7) | O(9)–W(2)–O(7) | 100.4(10) |
| O(8)–W(1)–O(3) | 100.8(5) | O(7)#2–W(2)–O(7) | 87.7(9) |
| O(6)–W(1)–O(3) | 91.1(5) | O(6)#1–W(2)–O(7) | 156.5(10) |
| O(8)–W(1)–O(4) | 99.7(5) | O(5)–W(2)–O(7) | 87.5(7) |
| O(6)–W(1)–O(4) | 86.5(4) | O(9)–W(2)–O(2) | 155.1(8) |
| O(3)–W(1)–O(4) | 159.4(5) | O(6)#1–W(2)–O(2) | 95.2(7) |
| O(8)–W(1)–O(5) | 101.2(6) | O(5)–W(2)–O(2) | 96.6(6) |
| O(6)–W(1)–O(5) | 156.4(6) | O(7)–W(2)–O(2) | 61.7(8) |
| O(3)–W(1)–O(5) | 89.0(4) | O(9)–W(2)–O(1) | 156.7(6) |
| O(4)–W(1)–O(5) | 85.2(4) | O(7)#2–W(2)–O(1) | 94.9(10) |
| O(8)–W(1)–O(1) | 167.1(6) | O(6)#1–W(2)–O(1) | 62.5(6) |
| O(6)–W(1)–O(1) | 89.2(6) | O(5)–W(2)–O(1) | 64.2(5) |
| O(3)–W(1)–O(1) | 85.2(6) | O(7)–W(2)–O(1) | 96.0(10) |
| O(4)–W(1)–O(1) | 74.3(5) | N(1)#3–Cu(1)–N(1) | 165.8(8) |
| O(5)–W(1)–O(1) | 67.3(5) | N(1)–Cu(1)–N(2) | 86.4(6) |
| O(9)–W(2)–O(7)#2 | 102.3(9) | N(1)–Cu(1)–N(2)#3 | 94.6(6) |
| O(9)–W(2)–O(6)#1 | 103.1(7) | N(2)–Cu(1)–N(2)#3 | 172.0(8) |
| O(7)#2–W(2)–O(6)#1 | 85.1(8) | N(1)–Cu(1)–O(1W) | 97.1(4) |
| O(9)–W(2)–O(5) | 99.8(6) | N(2)–Cu(1)–O(1W) | 86.0(4) |
| O(7)#2–W(2)–O(5) | 157.9(10) | O(1)#2–Si(1)–O(1) | 112.7(5) |
| O(6)#1–W(2)–O(5) | 90.9(6) | O(1)–Si(1)–O(2)#1 | 106.0(5) |

Symmetry codes: for **1** #1 $y$, $x$, $-z+3/2$; #2 $-x+y$, $-x$, $z$. for **2** #1 $y-1/3$, $x+1/3$, $-z+11/6$; #2 $-y+1$, $x-y+1$, $z$; #3 $y+2/3$, $x-2/3$, $-z+11/6$.

### 2.2. Syntheses

#### 2.2.1. Synthesis of $\{V^{IV}W^{VI}_{10}W^{V}_{2}O_{40}[Cu(en)_2(H_2O)]_3\}$ (**1**)

A mixture of $Na_2WO_4\cdot 2H_2O$ (0.658 g, 2 mmol), $CuSO_4\cdot 5H_2O$ (0.25 g, 1 mmol), $H_2C_2O_4\cdot 2H_2O$ (0.189 g, 1.5 mmol), $VOSO_4\cdot 2H_2O$ (0.201 g, 1 mmol) and $H_2O$ (15 mL) was mixed and stirred for 30 min, and the pH was adjusted to 8 with en. The resulting suspension was transferred to a Teflon-lined autoclave (25 mL) and kept at 180 °C for 3 days. After slow cooling to room temperature for 2 days, blue prism crystals were obtained by filtering, washing with distilled water, and drying in desiccators at ambient temperature. The yields were ca. 83% based on W. Elemental anal. Calcd. (%) for **1** $C_{12}H_{54}Cu_3N_{12}O_{43}VW_{12}$ (3502.34): C, 4.12; H, 1.55; N, 4.80. Found: C, 4.17; H, 1.59; N, 4.88.

#### 2.2.2. Synthesis of $\{SiW^{VI}_{10}W^{V}_{2}O_{40}[Cu(en)_2(H_2O)]_3\}$ (**2**)

The same procedure as that for **1** was followed except substituting $Na_2SiO_3\cdot 9H_2O$ (0.284 g, 1 mmol) for $VOSO_4\cdot 2H_2O$ (0.201 g, 1 mmol) in the reaction system. The black rhombohedron crystals were collected. Yield is 26% based on W. Elemental anal. Calcd (%) for **2** $C_{12}H_{54}Cu_3N_{12}O_{43}SiW_{12}$ (3479.58): C, 4.14; H, 1.56; N, 4.83. Found: C, 4.21; H, 1.64; N, 5.02.

### 2.3. X-ray crystallography

Intensity data were collected on a Bruker-AXS Smart CCD diffractometer with graphite-monochromated Mo$K\alpha$ ($\lambda = 0.71073$ Å) radiation at 293 K. The structures were solved by direct methods and refined using full-matrix least squares on $F^2$. All calculations were performed using the SHELXL-97 program package. In the final refinements [41], all atoms were refined anisotropically except for the O2 atoms of **1** and O1, O2 and O5 atoms of **2**, respectively, while no H atoms were included in the models. A summary of crystal data and structure refinement for compounds **1** and **2** are provided in Table 1. Selected bond lengths and angles of **1** and **2** are listed in Tables 2 and 3, respectively.

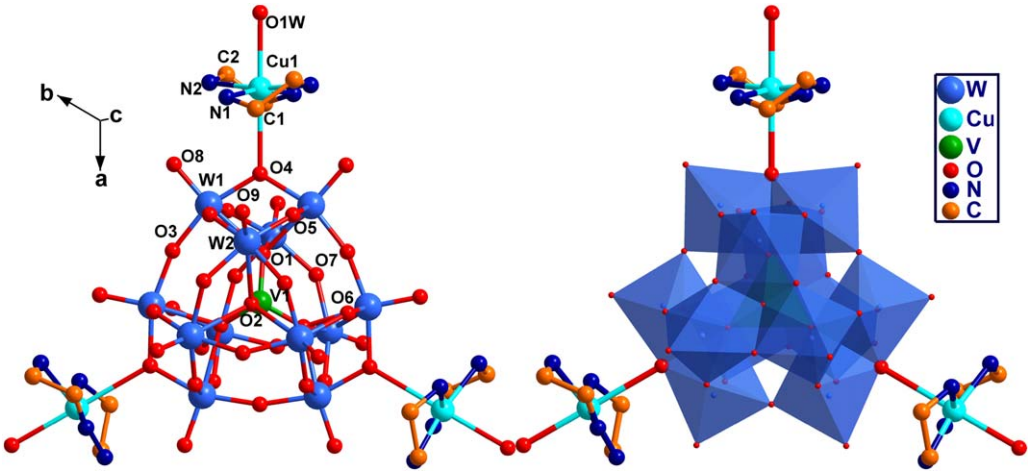


**Fig. 1.** Combined ball-and-stick (left) and polyhedral (right) representation of the neutral tri-supported POM: $\{V^{IV}W^{VI}_{10}W^{V}_{2}O_{40}[Cu(en)_2(H_2O)]_3\}$ (**1**).

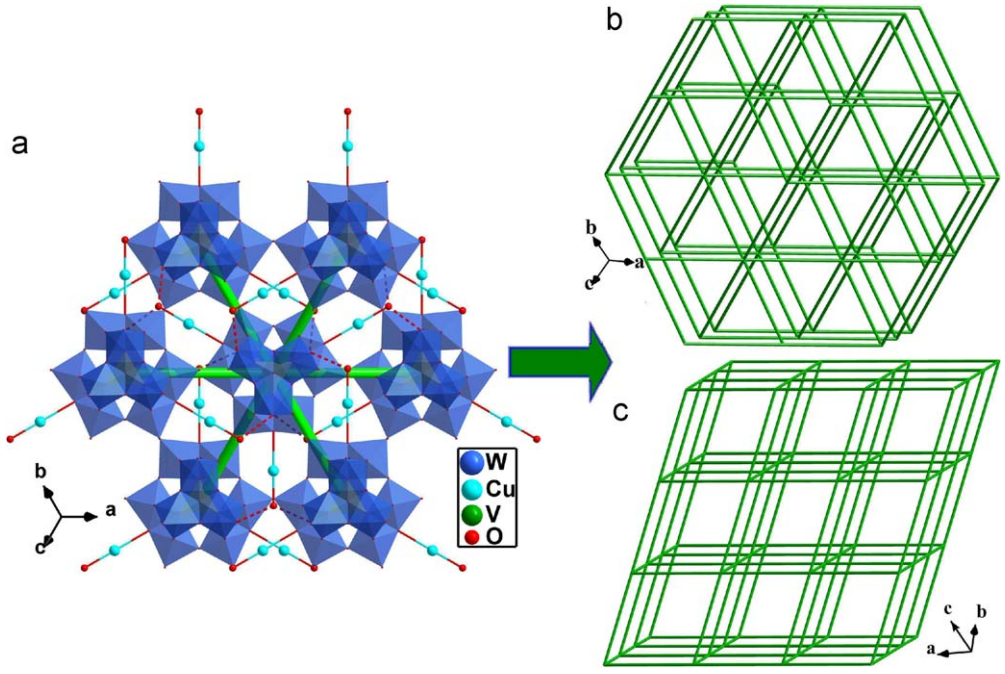


**Fig. 2.** (a) Supramolecular interactions occurred among $\{V^{IV}W^{VI}_{10}W^{V}_{2}O_{40}[Cu(en)_2(H_2O)]_3\}$ clusters and schematic view of the cluster as a 6-connected node (the C, N, H atoms are omitted for clarity, the O···O interactions shown as dotted lines), (b)/(c) schematic representation of the (6, 6)-connected 3D supramolecular framework in **1**.

## 3. Results and discussion

### 3.1. Syntheses

Two compounds were synthesized by using one-pot hydrothermal preparation. Hydrothermal synthesis has recently been proved to be a particularly powerful technique for the preparation of new organic–inorganic hybrid materials [42–45]. The exploitation of hydrothermal conditions provides a paradigm of shift from the thermodynamics to the kinetics such that equilibrium phases are replaced by structurally more complex metastable phases [42,43]. In the hydrothermal environment, the reduced viscosity of the solvent results in rate enhancement of solvent extraction of solids and crystal growth from solution. Furthermore, since different solubility problems can be minimized, a variety of organic and inorganic precursors can be introduced. Meanwhile, hydrothermal synthesis is still a relatively complex process because small changes in one or more of reaction factors, such as the kinds, concentrations, molar ratio of the reactants, pH values, reaction time, temperature, etc., may result in profound influence on final reaction products [44,45]. However, numerous successful experimental results from these so-called "black-box" reactions could suggest some preliminary synthetic experiences, which might be helpful for the improvement of further synthetic route.

For **1** and **2**, the synthesis of such controlled assembly based on tungsten-containing building units is generally difficult at room temperature (in contrast to corresponding molybdovanadate system) due to the kinetic sluggishness of tungsten. Consequently, compounds **1** and **2** were successfully prepared through hydrothermal reactions at the pH value of 8. No title compounds were obtained when the pH value of reaction system is larger than 8.5 and less than 7.5. This shows that preparation of **1** and **2** needs strictly control pH value of the reaction system. We tried to synthesize **1** and **2** under the same conditions without oxalic acid, but no desired crystal was found. So we consider that oxalic acid acts as reducing agent reducing $W^{VI}$ to $W^{V}$ in the synthesis reactions. Under other reaction condition being unchanged, crystal product of **1** was with lower yield obtained when $VOSO_4 \cdot 2H_2O$ was replaced with $V_2O_5$. We also tried to increase the yield of **2** through changing reaction factors, but we have not found the suitable reaction conditions. Compounds **1** and **2** are insoluble in water and common organic solvents (such as methanol, ethanol, ether, DMF and DMSO), and both of them are stable in atmosphere.

### 3.2. Crystal structures

Single-crystal X-ray diffraction analyses reveal that **1** and **2** are isomorphic with only slight differences in V replaced by Si, bond lengths and bond angles; compound **1** is described as an example below. As shown in Fig. 1, compound **1** shows a neutral tri-supported classical *psedo*-Keggin type structure where three $[Cu(en)_2(H_2O)]^{2+}$ fragments are supported on the novel tri-electron-reduced Keggin-type tungstovanadate $[V^{IV}W^{VI}_{10}W^{V}_{2}O_{40}]^{6-}$. The Keggin cluster $[V^{IV}W^{VI}_{10}W^{V}_{2}O_{40}]^{6-}$ is similar to that in $[Me_4N]_7[VW_{12}O_{40}] \cdot 15H_2O$ ($Me_4N$ = tetramethylammonium) reported by Khan [33]. The basic unit $[VW_{12}O_{40}]^{6-}$ may be viewed as a shell of $\{W_{12}O_{36}\}$ encapsulating a disordered $\{VO_4\}$ moiety, present at its center and responsible for the local tetrahedral geometry. The central V atom is surrounded by a cube of eight oxygen (six O1 and two O2) atoms with each of them half-occupied. Each oxygen of the $\{VO_4\}$ group, covalently bonded to three different tungsten centers of the shell, is in a $\mu_4$-bridging mode with V–$\mu_4$-O distances in the 1.629(9)–1.73(3) Å range and W–$\mu_4$-O distances in the 2.304(17)–2.455(17) Å range. The two independent tungsten centers in the heteropolyanion of **1** have essentially similar distorted octahedral environments defined by one terminal oxo-group with short W–O bond length [1.716(8), 1.696(8) Å], four doubly bridging oxo-groups with intermediate W–$\mu$-O bond lengths [1.877(16)–1.933(9) Å], and one $\mu_4$-O atom. W1 center completes its octahedron configuration by six oxygen atoms O1, O3, O4, O5, O6 and O8, and W2 center is surrounded by

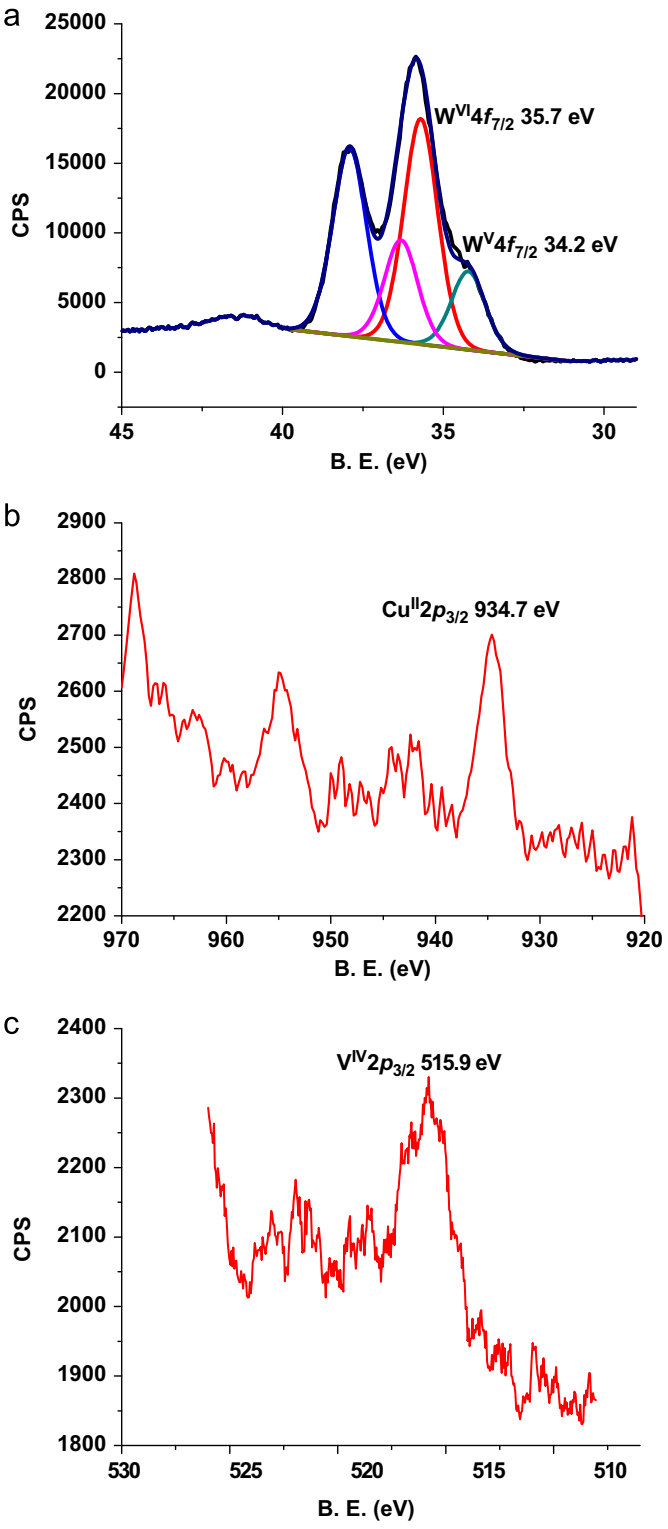


**Fig. 3.** The XPS for W (a), Cu (b) and V (c) in compound **1**.

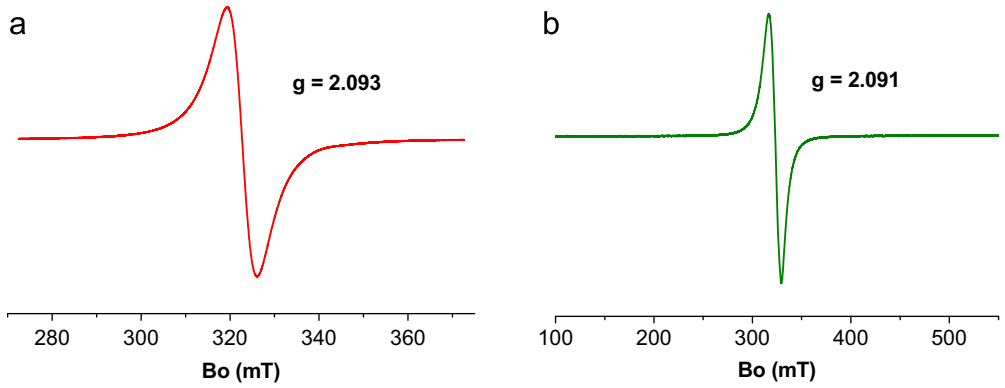


**Fig. 4.** The EPR spectra of **1** (a) and **2** (b).

O1, O5, O6, O9 and two O7 atoms. The three classes of W–O average distances in **1** (being 1.706, 1.898 and 2.367 Å, respectively) are comparable to the corresponding distances in $[H_4SiW_{12}O_{40}]$ (1.694, 1.901 and 2.372 Å) [46], $[VW_{12}O_{40}]^{7-}$ (1.708, 1.913, 2.326 Å) [33]. The selected bond distances and angles are compiled in Tables 2 and 3, respectively.

The most unusual structural feature of compound **1** is that each of three surface bridging oxygen atoms (O4) of the Keggin polyoxoanion $[VW_{12}O_{40}]^{6-}$ is coordinated to one $[Cu(en)_2(H_2O)]^{2+}$ fragment. To our knowledge, such a type of discrete Keggin polyoxoanion simultaneously supporting three TMCs has not been observed before. The Cu1 center possesses an elongated octahedral geometry defined by the bridging oxygen atom (Cu–O4, 2.740 Å) from the polyoxoanion, a coordination water molecule (Cu–O1W, 2.439(19) Å) *trans* to the bridging O4 atom and four N atoms from two en ligands with similar Cu–N bond distances in the range of 2.007(14)–2.028(16) Å. The bond lengths and angles at Cu1 are consistent with the Jahn–Teller active $d^9$ electronic configuration of divalent copper [47,48]. Another interesting structural feature of compound **1** is that the tri-supported POMs are extended into 3-D supramolecular network via hydrogen-bonding interactions between the terminal oxygen atoms (O9) and the coordinated water molecules (OW1) from neighboring POMs. As shown in Fig. 2, one $\{VW_{12}O_{40}[Cu(en)_2(H_2O)]_3\}$ cluster directly interacting its six adjacent neighboring clusters via strong hydrogen bondings [OW1⋯O9, 2.824(3) Å] can be regarded as a six connector leading to a classical distorted cubic (α-Po) net.

### 3.3. Characterization of compounds

#### 3.3.1. Bond valence sum (BVS), EPR spectra and XPS characterizations

According to elemental analyses, bond valence sums (BVS), coordination geometries, XPS spectra and charge balance, compound **1** is formulated as $\{V^{IV}W^{VI}_{10}W^{V}_{2}O_{40}[Cu(en)_2(H_2O)]_3\}$. The BVS [49] calculation result for the tungsten centers gives the values 5.67 for W1 and 6.04 for W2, which reveals that there exist 2 $W^V$ atoms and 10 $W^{VI}$ atoms in **1**. However, the BVS values of the tungsten centers and W–O distances do not clearly identify the reduced tungsten (V) sites. This is due to the possible delocalization of the *d* electrons of the reduced tungsten centers over the polyanion cluster framework involving all W as found in heteropolyblues, reduced hexamolybdate and hexatungstates [50–52]. In the almost ideal tetrahedron $\{VO_4\}$ (the O–V–O bond angle 109.0°), the average V–O distance (1.655 Å) is more longer than the corresponding bond distance in the fully oxidized Keggin-like isopolyvanadate $[V_{15}O_{42}]^{9-}$ [1.538(10) Å] [53] and also longer than the reduced cluster anion $[V^{IV}W_{12}O_{40}]^{7-}$ [1.628(7) Å] [33], indicating a reduced vanadium (IV) in **1** which is further confirmed by XPS result. To the best of our knowledge, the presence of the reduced $\{V^{IV}O_4\}$ group at the center of such a Keggin polyoxoanion is seldom seen [33,35]. The XPS for **1** (Fig. 3) show a peak at 515.9 eV attributed to $V^{IV}2p_{3/2}$, one peak at 934.7 eV ascribed to $Cu^{II}2p_{3/2}$ and along with two overlapped peaks at 34.2 and 35.7 eV attributed to $W^V4f_{7/2}$ and $W^{VI}4f_{7/2}$, respectively. The EPR spectrum for **1** (Fig. 4a) recorded at room temperature (298 K) on a crystalline sample show the $Cu^{II}$ signal with $g = 2.093$, being consistent with the results of structure analyses. As far as we know, up to now, compound **1** is the first example of tri-supported classical Keggin POM possessing discrete structure.

The relative bond lengths and bond angles of **2** are comparable to those of **1** (Tables 2 and 3). The BVS calculation of **2** suggests that the valencies of all the atoms are also very similar to that in **1**. The EPR spectrum of **2** exhibits the $Cu^{II}$ signal at 293 K with $g = 2.091$ (Fig. 4b). The XPS for **2** (Fig. 5) give a peak at 104.4 eV attributed to $Si^{IV}2p_{3/2}$, one peak at 935.2 eV ascribed to $Cu^{II}2p_{3/2}$ and two overlapped peaks at 33.9 and 35.8 eV attributed to $W^V4f_{7/2}$ and $W^{VI}4f_{7/2}$, respectively. All of these results further confirm ones of the structure analyses.

#### 3.3.2. Infrared spectra and UV–Vis solid diffuse reflection spectrum

In the low-wavenumber region ($\nu < 1100\,cm^{-1}$) of the IR spectrum (Fig. S1) for **1**, there are four characteristic asymmetric vibration peaks resulting from the Keggin structure, namely, $\nu$(V–Oc), $\nu$(W–Ot), $\nu$(W–Ob) and $\nu$(W–Oc) appearing at 1043, 947, 871 and 775 $cm^{-1}$, respectively. For **2**, the strong bands at 1040, 951, 898 and 769 $cm^{-1}$ should be attributed to $\nu$(Si–Oc), $\nu$(W–Ot), $\nu$(W–Ob) and $\nu$(W–Oc), respectively. The strong broad bands around 3434 $cm^{-1}$ for **1** and 3443 $cm^{-1}$ for **2** could be due to stretching vibration of water molecules, and the absorption bands at 1623 $cm^{-1}$ for **1** and 1617 $cm^{-1}$ for **2** correspond to the deformation vibration of water molecules. Peaks in the 3300–2900 $cm^{-1}$ region are attributed to stretching vibrations of N–H and C–H bonds, and peaks in the range of 1500–1100 $cm^{-1}$ are characteristic of C–N bonds in en [21,33,35,37]. The UV–Vis solid diffuse reflection spectrum (Fig. S2) of **1** exhibits a medium intensity peak at 249 nm is associated with the O–W LMCT band, whereas the strong wide band 436–610 nm is due to the Cu–N and $Cu–O_{(POM)}$ LMCT bands, and another peak at 640 nm with its tail extending to 800 nm is attributed to overlap of two bands of the intervalence transition from $W^V$ to $W^{VI}$ by the W–O–W bond and the *d*–*d* transitions of $W^V$ octahedra [3,12,54].

#### 3.3.3. Magnetism property

The structure of reduced POMs supported by $[Cu(en)_2]^{2+}$ in the compounds allows us to predict the existence of magnetic exchange coupling. The variable temperature magnetic susceptibility

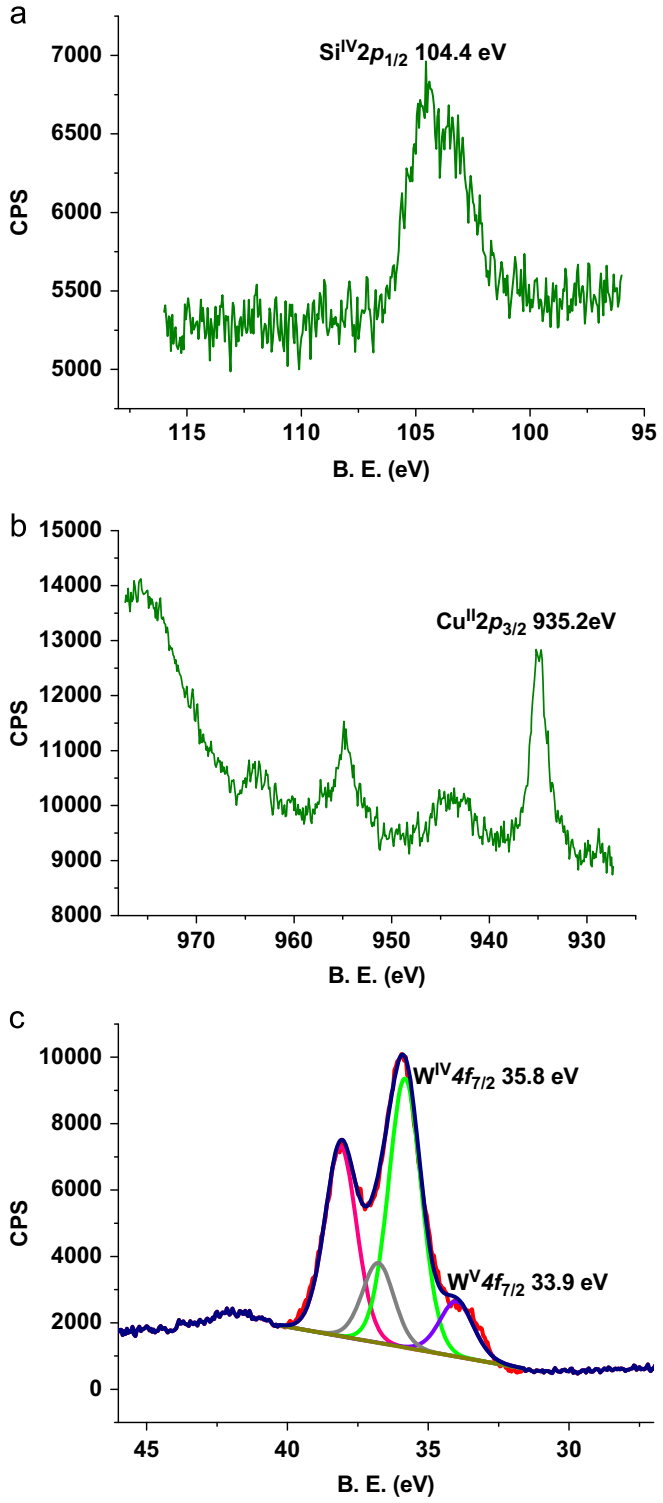


**Fig. 5.** The XPS for Si (a), Cu (b) and W (c) in compound **2**.

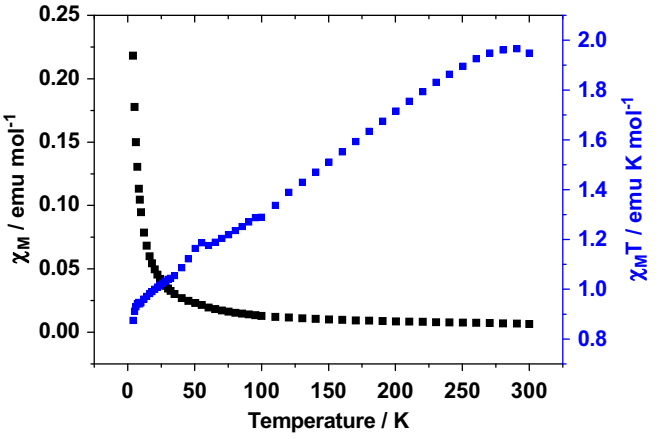


**Fig. 6.** Temperature dependences of $\chi_M$ and $\chi_M T$ for **1**.

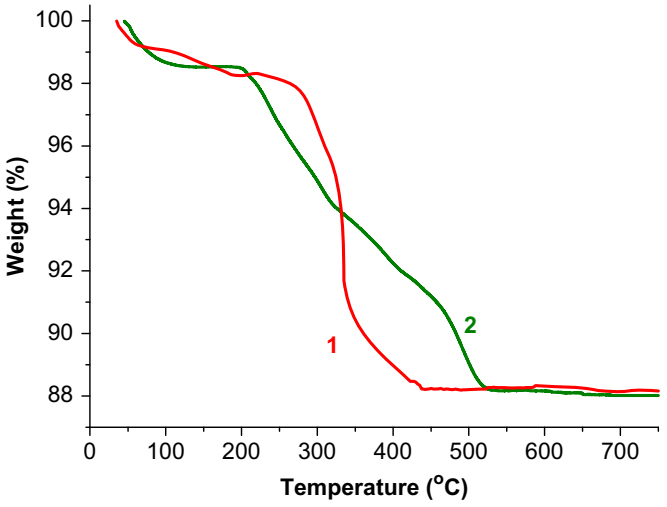


**Fig. 7.** TG curves of compounds **1** and **2**.

of **1** was measured between 4 and 300 K at 1000 Oe. The product $\chi_m T$, where $\chi_m$ is the molar magnetic susceptibility in terms of the unit formula, continuously decreased as the temperature is lowered, indicating the presence of antiferromagnetic exchange coupling (Fig. 6). The observed value at room temperature ($\chi_M T = 1.97$ emu K mol$^{-1}$, $\mu_{eff} = 3.97\,\mu_B$) is slightly smaller than theoretical value of one uncoupled $S = \frac{1}{2}$ spins of V$^{IV}$ atoms, three uncoupled $S = \frac{1}{2}$ spins of Cu$^{II}$ atoms and two uncoupled $S = \frac{1}{2}$ spins of W$^{V}$ atoms ($\chi_M T = 2.25$ emu K mol$^{-1}$, $\mu_{eff} = 4.24\,\mu_B$). The magnetic data of compound **1** obey the Curie–Weiss law in the range 50–300 K temperature region, and gives values $C = 2.01$ emu mol$^{-1}$ K and $\theta = -29.76$ K, characteristic of the antiferromagnetic interactions of **1**. Unfortunately, no suitable theoretical model is available in the literature [55] for such a complex system.

### 3.3.4. *Thermogravimetric analyses*

TG curves of **1** and **2** all show two major steps of weight losses (Fig. 7). The first weight loss of **1** corresponds to the release of three coordinated water molecules (calcd. weight loss 1.54%; found 1.69%) at relatively lower temperature (below ~150 °C). The remainder stages of **1** (in the range 220–450 °C) are attributed to the decomposition of the organic ligand en (calcd. weight loss 10.30%; found 10.08%). For **2**, the weight loss amounts to 1.49% (45–130 °C) and 10.38% (190–530 °C), respectively. The calculated weight losses for three coordination water molecules (1.56%) and six en molecules (10.36%) are in agreement with the results of the TG experiment. The final products are $WO_3$, $V_2O_5$ and CuO for **1**, $WO_3$, $SiO_2$ and CuO for **2**. The experimental total weight losses (11.77% for **1** and 11.87% for **2**) are in good agreement with the calculated weight losses (11.15% for **1** and 11.46% for **2**).

## 4. Conclusion

In conclusion, we have prepared and characterized two interesting 3-D supramolecular architectures based on the novel neutral tri-supported Keggin units $\{XW_{12}O_{40}[Cu(en)_2(H_2O)]_3\}$ ($X = V$, Si). They represent the first example of tri-supported classical Keggin POMs possessing discrete structure. The magnetic properties of **1** have also been studied, and its magnetic susceptibility obeys Curie–Weiss law, showing antiferromagnetic coupling. The successful isolation of compounds **1** and **2** confirms that the activation of surface oxygen atoms of POMs by introducing strong reducing regents would be a feasible and promising synthetic route to decorate POMs with various organic groups and TMC moieties.

## Supplementary data

CCDC numbers 713787 and 713788 contain the supplementary crystallographic data for **1** and **2**, respectively. These data can be obtained free of charge via http://www.ccdc.cam.ac.uk/conts/retrieving.html, or from the Cambridge Crystallographic Data Centre, 12 Union Road, Cambridge CB2 1EZ, UK; fax: +44 1223 336 033; or e-mail: deposit@ccdc.cam.ac.uk. IR spectra and UV–Vis solid diffuse reflection spectrum for **1** and **2** are presented in the Supporting Information.

## Acknowledgment

This work was supported by the National Natural Science Foundation of China (no. 20571021).

## Appendix A. Supplementary material

Supplementary data associated with this article can be found in the online version at doi:10.1016/j.jssc.2009.05.030.

## References

[1] C.L. Hill, Chem. Rev. Polyoxometalates 98 (1998) 1.
[2] M.T. Pope, A. Müller, Polyoxometalates: From Platonic Solids to Anti-Retro Viral Activity, Kluwer Academic Publishers, Dordrecht, The Netherlands, 1994.
[3] M.T. Pope, Heteropoly and Isopoly Oxometalates, Springer, New York, 1983.
[4] P. Mialane, A. Dolbecq, L. Lisnard, A. Mallard, J. Marrot, E. Rivière, F. Sécheresse, Angew. Chem. Int. Ed. 41 (2002) 2398.
[5] H.Y. An, D.R. Xiao, E.B. Wang, Y.G. Li, Z.M. Su, L. Xu, Angew. Chem. Int. Ed. 45 (2006) 904.
[6] M.L. Wei, C. He, W.J. Hua, C.Y. Duan, S.H. Li, Q.J. Meng, J. Am. Chem. Soc. 128 (2006) 13318.
[7] S.X. Liu, L.H. Xie, B. Gao, C.D. Zhang, C.Y. Sun, D.H. Li, Z.M. Su, Chem. Commun. (2005) 5023.
[8] C.D. Wu, C.Z. Lu, H.H. Zhuang, J.S. Huang, J. Am. Chem. Soc. 124 (2002) 3836.
[9] A. Müller, S.Q.N. Shah, H. Bögge, M. Schmidtmann, Nature 397 (1999) 48.
[10] U. Kortz, M.G. Savelieff, F.Y. Abou Ghali, L.M. Khalil, S.A. Maalouf, D.I. Sinno, Angew. Chem. Int. Ed. 41 (2002) 4070.
[11] W.B. Yang, X. Lin, C.Z. Lu, H.H. Zhuang, J.S. Huang, Inorg. Chem. 39 (2000) 2706.
[12] K. Yu, Y.G. Li, B.B. Zhou, Z.H. Su, Z.F. Zhao, Y.N. Zhang, Eur. J. Inorg. Chem. (2007) 5662.
[13] B.S. Bassil, S.S. Mal, M.H. Dickman, U. Kortz, H. Oelrich, L. Walder, J. Am. Chem. Soc. 130 (2008) 6696.
[14] U. Kortz, F. Hussain, M. Reicke, Angew. Chem. Int. Ed. 44 (2005) 3773.
[15] S.T. Zheng, J. Zhang, G.Y. Yang, Angew. Chem. Int. Ed. 47 (2008) 3909.
[16] J.Y. Niu, P.T. Ma, H.Y. Niu, J. Li, J.W. Zhao, Y. Song, J.P. Wang, Chem. Eur. J. 13 (2007) 8739.
[17] X.B. Cui, J.Q. Xu, H. Meng, S.T. Zheng, G.Y. Yang, Inorg. Chem. 43 (2004) 8005.
[18] Q. Chen, C.L. Hill, Inorg. Chem. 35 (1996) 2403.
[19] Y. Xu, H.G. Zhu, H. Cai, X.Z. You, Chem. Commun. 1 (1999) 787.
[20] W.B. Yang, C.Z. Lu, X.P. Zhan, H.H. Zhuang, Inorg. Chem. 41 (2002) 4621.
[21] C.M. Liu, D.Q. Zhang, M. Xiong, D.B. Zhu, Chem. Commun. (2002) 1416.
[22] L.M. Duan, C.L. Pan, J.Q. Xu, X.B. Cui, F.T. Xie, T.G. Wang, Eur. J. Inorg. Chem. (2003) 2578.
[23] H.N. Miras, D.J. Stone, E.L. Mclnnes, R.G. Raptis, P. Baran, G.I. Chilas, M.P. Siqalas, T.A. Kabanos, L. Cronin, Chem. Commun. (2005) 4703.
[24] Y. Xu, J.Q. Xu, K.L. Zhang, X.Z. You, Chem. Commun. (2000) 153.
[25] S. Reinoso, P. Vitoria, L.S. Felices, L. Lezama, J.M. Gutiérrez-Zorrilla, Inorg. Chem. 45 (2006) 108.
[26] J.Y. Niu, Z.L. Wang, J.P. Wang, Inorg. Chem. Commun. 6 (2003) 1272.
[27] Y. Lu, Y. Xu, E.B. Wang, J. Lü, C.W. Hu, L. Xu, Cryst. Growth Des. 5 (2005) 257.
[28] C.M. Liu, D.Q. Zhang, D.B. Zhu, Cryst. Growth Des. 3 (2003) 363.
[29] M. Yuan, Y.G. Li, E.B. Wang, C.G. Tian, L. Wang, C.W. Hu, N.H. Hu, H.Q. Jia, Inorg. Chem. 42 (2003) 3670.
[30] G.Y. Luan, Y.G. Li, S.T. Wang, E.B. Wang, Z.B. Han, C.W. Hu, N.H. Hu, H.Q. Jia, J. Chem. Dalton Trans. (2003) 233.
[31] S. Reinoso, P. Vitoria, L. Lezama, A. Luque, J.M. Gutiérrez-Zorrilla, Inorg. Chem. 42 (2003) 3709.
[32] Z.Z. Han, Y.L. Zhao, J. Peng, H.Y. Ma, Q. Liu, E.B. Wang, N.H. Hu, H.Q. Jia, Eur. J. Inorg. Chem. (2005) 264.
[33] M.I. Khan, S. Cevik, R. Hayashi, J. Chem. Soc. Dalton Trans. (1999) 1651.
[34] V. Shivaiah, S. Hajeebu, S.K. Das, Inorg. Chem. Commun. 5 (2002) 996.
[35] Y.B. Liu, L.M. Duan, X.M. Yang, J.Q. Xu, Q.B. Zhang, Y.K. Lu, J. Liu, J. Solid State Chem. 179 (2006) 122.
[36] Y. Xu, L.B. Nie, G.N. Zhang, Q. Chen, X.F. Zheng, Inorg. Chem. Commun. 9 (2006) 329.
[37] J. Liu, J.N. Xu, Y.B. Liu, Y.K. Lu, J.F. Song, X. Zhang, X.B. Cui, J.Q. Xu, T.G. Wang, J. Solid State Chem. 180 (2007) 3456.
[38] J.P. Wang, S.Z. Li, Y. Shen, J.Y. Niu, Cryst. Growth Des. 8 (2008) 372.
[39] L. Lisnard, A. Dolbecq, P. Mialane, J. Marrot, E. Rivière, S.A. Borshch, S. Petit, V. Robert, C. Duboc, T. McCormac, F. Sécheresse, Dalton Trans. (2006) 5141.
[40] C.P. Pradeep, D.L. Long, G.N. Newton, Y.F. Song, L. Cronin, Angew. Chem. Int. Ed. 47 (2008) 4388.
[41] G.M. Sheldrick, SHELXTL 97, Program for Crystal Structures Solution and Refinement, University of Göttingen, Germany, 1997.
[42] P.J. Hagrman, D. Hagrman, J. Zubieta, Angew. Chem. Int. Ed. 38 (1999) 2638.
[43] S.H. Feng, R.R. Xu, Acc. Chem. Res. 34 (2001) 239.
[44] P.M. Forster, A.R. Burbank, C. Livage, G. Férey, A.K. Cheetham, Chem. Commun. (2004) 368.
[45] P.Q. Zheng, Y.P. Ren, L.S. Long, R.B. Huang, L.S. Zheng, Inorg. Chem. 44 (2005) 1190.
[46] J.Y. Niu, X.Z. You, C.Y. Duan, H.K. Fun, Z.Y. Zhou, Inorg. Chem. 35 (1996) 4211.
[47] S. Noro, R. Kitaura, M. Kondo, S. Kitagawa, T. Ishii, H. Matsuzaka, M. Yamashita, J. Am. Chem. Soc. 124 (2002) 2568.
[48] M.R. Montney, R.L. LaDuca, J. Solid State Chem. 181 (2008) 828.
[49] I.D. Brown, in: M. O'Keefe, A. Navrotsky (Eds.), Structure and Bonding in Crystals, vol. 2, Academic Press, New York, 1981, pp. 1–30.
[50] M.T. Pope, A. Müller, Angew. Chem. Int. Ed. 30 (1991) 34.
[51] N. Casan-Pastor, L.C.W. Baker, J. Am. Chem. Soc. 114 (1992) 10384 and references therein.
[52] M.I. Klan, S. Cevik, R.J. Doedence, Q. Chen, S. Li, C.J. O'connor, Inorg. Chem. Acta 277 (1998) 69.
[53] D. Hou, K.S. Hagen, C.L. Hill, J. Chem. Soc. Chem. Commun. (1993) 426.
[54] B. DasGupta, C. Katz, T. Israel, M. Watson, L. Zompa, Inorg. Chim. Acta 292 (1999) 172.
[55] O. Kahn, Molecular Magnetism, VCH, New York, 1993.